Catalysis Science & Technology

Accepted Manuscript

This article can be cited before page numbers have been issued, to do this please use: T. Yu, J. Wang, M. Shen and W. Li, *Catal. Sci. Technol.*, 2013, DOI: 10.1039/C3CY00453H.

Cite this: DOI: 10.1039/c0xx00000x

www.rsc.org/xxxxxx

ARTICLE TYPE

The NH_3-SCR over Cu/SAPO-34 catalysts with various acid contents at low Cu loading

Tie Yu,[a] Jun Wang,[a] Meiqing Shen,*[a,b] and Wei Li[c]

Received (in XXX, XXX) Xth XXXXXXXXX 20XX, Accepted Xth XXXXXXXXX 20XX

DOI: 10.1039/b000000x

The four Cu/SAPO-34 catalysts are used to research the effect of acid contents on the NH_3-SCR activity through changing the Si amounts. Though the catalysts contain the similar Cu loading by ion-exchange method, they perform different NO conversions during 120-600 °C. The NH_3-TPD results show that the Si amounts can adjust the acid contents of SAPO-34. During the low temperature range, the kinetic tests prove that the various acid contents could not affect the apparent activation energy (Ea) of Selective Catalytic Reduction by NH_3 (NH_3-SCR) over Cu/SAPO-34. But it is found that the acid densities are related to the NO conversions at low temperature. During the high temperature range, the increment of acid contents in Cu/SAPO-34 catalysts inhibits the NH_3 conversions in the NH_3 Oxidation results. And NH_3 Oxidation and NH_3-SCR are competing reactions and the former one can decrease the NO conversions. Finally, the influence of acid contents on the NH_3 Oxidation is also investigated by the kinetic tests.

1 Introduction

NO*x* is one of the most hazardous greenhouse gases, which can cause human lung disease, photochemical smog and acid rain[1]. Recently, more and more strict regulations are implemented to control the NO*x* emission from the stationary source and mobile source, especially exhaust gas of vehicle. Since the NH_3-SCR technology was firstly applied in 1970s, it had become one of the most effective methods to decrease the NO*x* emission. The NH_3-SCR technology utilizes the NH_3 as reductant to remove NO*x* as following: $4\ NH_3+4\ NO+ O_2=4\ N_2+6\ H_2O$[2-4].

The SCR zeolites catalysts have been widely applied for their higher NO conversions and wider temperature windows than the oxide catalysts and noble metal catalysts[2,5]. Recently, Cu/chabazite (CHA) catalysts have become another focus in SCR research due to its excellent hydrothermal stability and N_2 selectivity[6]. SAPO-34 and SSZ-13, small pore sized molecular sieves with CHA structure, are built from infinite TO_4 tetrahedral units (T = Si, Al for SSZ-13 and Si, Al, and P for SAPO-34) with the same topology[7]. Kwak[8] reported that the Cu-SSZ-13 presented the higher NO conversion and the less byproducts (NO_2/N_2O) concentrations than Cu/ZSM-5 and Cu/beta. Moreover, their further research found that the stable CHA structure ensure the superior SCR activities of the aged Cu-SSZ-13 catalysts, while the Cu/ZSM-5 and Cu/beta showed decreased NO conversions due to the structure collapse by water in hydrothermal treatment[9]. Meanwhile, Fickel[6] also studied the small-pore Cu/CHA catalysts, which also showed higher NO conversions and excellent hydrothermal stability than medium-pore zeolites. Our previous works[10,11] about the Cu/CHA catalysts had proved that the Cu^{2+} species were the active sites for NH_3-SCR over Cu/SAPO-34 at low temperature, and hydrothermal treatments benefited the improvement of NO conversion due to the increments of Cu^{2+} species. Furthermore, it is known that the Si amounts can affect the acid contents of SAPO-34 and the acidity played an important role in NH_3-SCR over Cu/SAPO-34[10]. However, there have not been evident conclusions about the relation between the acid contents and the activities at the whole temperature range, and the influence of acid contents on the SCR mechanism is not verified.

In this work, the main aim is to further investigate the effect of acid contents on the SCR activities and NH_3 oxidation over Cu/SAPO-34 catalysts. Firstly, four SAPO-34 supports with various Si contents are synthesized and the Cu/SAPO-34 catalysts are prepared using ion-exchange method with equivalent Cu loading by precise control of the process. The XRD, SEM are used to check the chabazite structure of catalysts. Secondly, the NH_3-TPD and NH_3 storage tests are performed to analyze the various acidities of zeolites. In addition, the kinetic tests and the NH_3 Oxidation experiments are used to explore the influence of acid contents on the SCR activities at different temperature ranges and the competition of the NH_3-SCR/NH_3 Oxidation over Cu/SAPO-34. Finally, the relationships between the acidities and the SCR activities/NH_3 oxidation are conducted for different temperature ranges.

2 Experimental

2.1 The preparation of SAPO-34 and Cu/SAPO-34

The SAPO-34 was synthesized with the mole composition of 0.2 Morpholine (MA): 0.1 Al_2O_3: 0.1 P_2O_5: (0.02-0.15) SiO_2: 6.5 H_2O by hydrothermal method. The sources of Si, P, and Al were silica sol, 85% phosphoric acid and pseudoboehmite, respectively. Firstly, the phosphoric acid and the pseudoboehmite were mixed with H_2O, and the mixture was fiercely stirred for 1 h. Then the silica sol and the MA were added and blended well. Thirdly, the

View Article Online
DOI: 10.1039/C3CY00453H

homogeneous mixture was sealed in autoclave and heated at 200 °C for 24 h. After crystallization, the as-synthesized sample was obtained through centrifuging, washing and drying at 100 °C for 6 h. Finally, the samples were calcined in air (300 ml/min) from 30 °C to 650 °C under the rate of 3 °C/min and stayed at 650 °C for 6 h. The compositions of SAPO-34 were tested by x-ray fluorescence spectrometer (XRF) in Table 1 and the molecular sieves were denoted as Si*x*, where *x* represented additive ratios of the silica sol.

The preparation of Cu/SAPO-34 contained two steps by ion-exchange method. Firstly, the NH_4-SAPO-34 was obtained by exchanging HSAPO-34 in ammonium nitrate solution at 80 °C for 3 h. Then the NH_4-SAPO-34 was stirred with copper sulfate solution to obtain Cu/SAPO-34. The exchange times for various supports were precisely controlled to get equivalent Cu loading. After each ion-exchange processes, the slurry was filtered, washed and the solid was dried at 90-100 °C for 16 h in oven. And then the dried Cu/SAPO-34 was calcined at 550 °C for 4 h in muffle furnace. The Cu loading over catalysts were tested by ICP and the results were shown in Table 1. The Cu/SAPO-34 was named as Cu/Si*x* for short.

2.2 The SCR activities

The SCR activity was tested in a quartz reactor (20 mm inner diameter) using 0.1 g sample (60-80 mesh) mixed with 0.9 g quartz (60-80 mesh) at atmospheric pressure. The catalyst was sealed in the tube with quartz wool. The temperature was controlled by a type K thermocouple inserted into the center of the power catalyst. The Fourier Transform Infrared (FTIR) spectrometer (MKS-2030) equipped with a 5.11 m gas cell was used to measure the concentration of NO, NO_2, N_2O and NH_3. The gas flow rates in all experiments were controlled at 500 ml/min. Prior to the experiment, the catalysts were heated up to 500 °C and kept at 500 °C for 10 min under 5% O_2 in N_2. Steady-state activity tests were performed for all catalysts using a feed gas composition of 500 ppm NO, 500 ppm NH_3 and 5% O_2. In addition, the SCR tests with 3% H_2O and 6% CO_2 were also performed and the results were shown in the Fig .S6. The tested temperature was from 120 °C to 600 °C. The NO conversion was calculated as following equation:

$$\text{NO conversion [\%]} = \frac{NO_{inlet} - NO_{outlet}}{NO_{outlet}} \times 100\ [\%] \qquad (1)$$

2.3 The characterization of zeolites

The XRD patterns were performed using X'Pert Pro diffractometer operating at 40 kV and 40 mA with nickel-filtered Cu Kα radiation (λ=1.5418 Å) in the range 5°< 2θ < 50° with a step size of 0.02 °. The BET surface area (m^2/g) was determined from the liner portion of the BET plot by measuring the N_2 isotherm of the samples at 77 K using F-Sorb 3400 volumetric adsorption/desorption apparatus. Prior to the measurement, the zeolites were degassed at 150 °C under vacuum for 3 h.

Scanning Electron Microscopy (SEM) image of the samples was measured on a HITACHI S4800 field emission microscope. The samples were pasted on a sample holder using a carbon tape and then covered with Pt film to become conductive. SEM images were taken at magnifications of 2,000 with the 3 kV electron beam.

Temperature Programmed Desorption by NH_3 (NH_3-TPD) experiments were performed to evaluate the acid contents over samples. Prior to the experiments, the catalysts were pretreated at 500 °C for 30 min in 5% O_2/N_2, and then cooled to 80 °C in N_2. NH_3 adsorption was in 500 ppm NH_3/N_2 until the outlet NH_3 concentration was stable. Then, the catalysts were purged with N_2 to remove any weakly absorbed NH_3 at 80 °C. Finally, the catalysts were heated from 80 °C to 550 °C at a ramping rate of 10 °C /min.

The NH_3/NO oxidation were performed in the equivalent reactor, the ways of packing and the pretreatment with SCR tests. The inlets contained: 500 ppm NH_3/NO and 5% O_2/N_2. The gas flow and the volume hourly space velocity in all experiments were controlled at 500 ml/min and 300,000 h^{-1}, respectively. The NH_3 oxidation was performed from 150 °C to 550 °C, while the NO oxidation was performed from 120 °C to 600 °C.

The Electron Paramagnetic Resonance (EPR) spectra were recorded on a Bruker ESP320 spectrometer. The Bruker ESP320E software and the special Bruker program were used for data analysis. The EPR spectra were recorded at room temperature and atmospheric pressure. In order to observe the hyperfine structure of Cu^{2+} species, dehydration of the samples was carried out prior to EPR experiments. The Cu/SAPO-34 catalysts were vacuumed at 4.0×10^{-4} Pa for 1 h at 120 °C.

2.4 The Kinetic Measurements

The NH_3-SCR kinetic tests were performed in a thin quartz tube using 25 mg catalyst and 125 mg quartz sand. A relative small particles sizes (80-100 mesh) and volume hourly space velocity (3,600,000 h^{-1}) ensured the elimination of internal and external diffusion respectively. Prior to the kinetic experiments, the samples were pretreated in 5% O_2/N_2 at 500 °C. The inlets consisted of 500 ppm NO, 500 ppm NH_3, 5% O_2 with N_2 as the balance. The kinetic steady-state measurements were obtained from 150 °C to 225 °C. By assuming plug flow reactor and free of diffusion limitations, the NH_3-SCR reaction rates can be calculated from the NO_x conversion by:

$$\text{rate}\,[\text{mol NO}_x \cdot \text{g}_{cata} \cdot \text{s}^{-1}] = \frac{X_{NO_x}[\%] \times F_{NO_x}[\text{L}_{(NO_x)} \cdot \text{min}^{-1}]}{m_{cata} \times 60[\text{s} \cdot \text{min}^{-1}] \times 22.4[\text{L} \cdot \text{mol}^{-1}]}\ [\text{mol NO}_x \cdot \text{g}_{cata} \cdot \text{s}^{-1}] \qquad (2)$$

X_{NOx} = NO_x Conversion, [%];

F_{NOx} = Flow Rate of NO_x, [$L_{(NOx)}$ min^{-1}]

The NH_3 Oxidation kinetic experiments were conducted under the same condition with the NH_3-SCR. The inlets consisted of 500 ppm NH_3, 5% O_2 with N_2 as the balance. The kinetic steady-state measurements were obtained from 410 °C to 490 °C.

3 Results and Discussion

3.1 The characterization of zeolites

The composition of SAPO-34 is shown in Table 1. It is seen that the four molecular sieves only show obvious difference of Si amounts which can be adjusted by the additive amount of silica sol in the materials. In addition, the four Cu/SAPO-34 catalysts

View Article Online
DOI: 10.1039/C3CY00453H

present the similar Cu loading due to precise process control.

The XRD results

The XRD profiles in Fig. 1 present that the four SAPO-34 supports all have the typical CHA structure[12,13]. In addition, the peak intensities deducting the background are compared in Fig. S1 (supplementary information) and they increase with the increment of Si contents, which is mainly due to the higher crystallinity for Si1.4 and Si1.0[14,15].

Table 1 the composition of SAPO-34 supports and Cu/SAPO-34 catalysts

The catalysts	The materials ratios *[a]	The molecular sieve *[b]	The crystal size (μm)	The Cu loading (wt%)
Cu/Si0.2	1:1:0.2	$Si_{0.08}Al_{0.45}$	8-10	0.89
Cu/Si0.6	1:1:0.6	$Si_{0.13}Al_{0.44}$	4-6	0.89
Cu/Si1.0	1:1:1	$Si_{0.15}Al_{0.43}$	4-6	0.90
Cu/Si1.4	1:1:1.4	$Si_{0.18}Al_{0.42}$	2-4	0.94

*[a]: the mole ratio of Al_2O_3:P_2O_5:SiO_2.

*[b]: the P ratios in $Si_xAl_yP_zO_2$ were omitted as Si_xAl_y for abbreviation. During the formula of $Si_xAl_yP_zO_2$, $(x + y + z) = 1$.

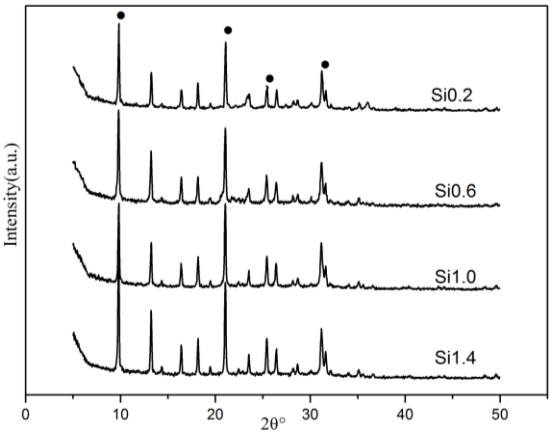

Fig. 1 the XRD profiles of SAPO-34 supports

The BET results

The BET results in Table 2 illustrate that the composition of SAPO-34 can affect their specific surface area (SSAs). The Si0.2 has smaller SSA than others, which is due to its lower crystallinity. Besides, the SAPO-34 supports show the equivalent SSAs with that of the corresponding Cu/SAPO-34, which reflects that the loading of Cu dose not change the SSA of SAPO-34 supports.

Table 2 the specific surface area (SSA) of samples

The catalysts	The SSA of supports (m^2/g)	The SSA of catalysts (m^2/g)
Cu/Si0.2	447.6	447.1
Cu/Si0.6	590.9	598.4
Cu/Si1.0	635.9	634.5
Cu/Si1.4	550.6	547.1

The SEM results

The SEM results in Fig. 2 show that the four SAPO-34 supports have the representative cubic structure of CHA[12,13], which consists with the XRD results. In addition, the four SAPO-34 supports present a decreasing crystal sizes in Table 1 when the Si contents increase. The decline of crystal sizes may be due to a small number of Si islands[16]. The SAPO-34 is considered to be synthesized by the substitution of P atoms in AlPOs molecular sieves by Si[17]. If the mole ratio of the (Si + P)/Al is not bigger than 1, Si atom substitutes P and forms the Si (4OAl) species. If the ratio of (Si + P)/Al is bigger than 1, the substitution of adjacent P and Al by Si atoms occurs and the Si islands appear as the coordination structure of Si (nOAl, n=0-3)[12,17]. And this structure defects can inhibit the growth of molecular sieves. Furthermore, the (Si + P)/Al values for the four supports are listed in Table S1 (the supplementary information). It is seen that the (Si + P)/Al value increases with the increment of Si amount in SAPO-34. Due to this law, the ^{29}Si NMR spectra of Si0.2 and Si1.4 are conducted in Fig. S7. The Si islands form in Si1.4 due to its highest (Si + P)/Al value and the Si0.2 almost presents no Si islands peaks for its lowest (Si + P)/Al value. Similarly, it is conducted that the proportion of Si islands in four SAPO-34 molecular sieves improves with the raise of (Si + P)/Al value. Therefore, the increment of Si amounts may cause the reduction of crystal sizes due to the more Si islands. Meanwhile, the same SEM images of Cu/SAPO-34 and corresponding supports also present that the loading of Cu dose not influence the structure of zeolites.

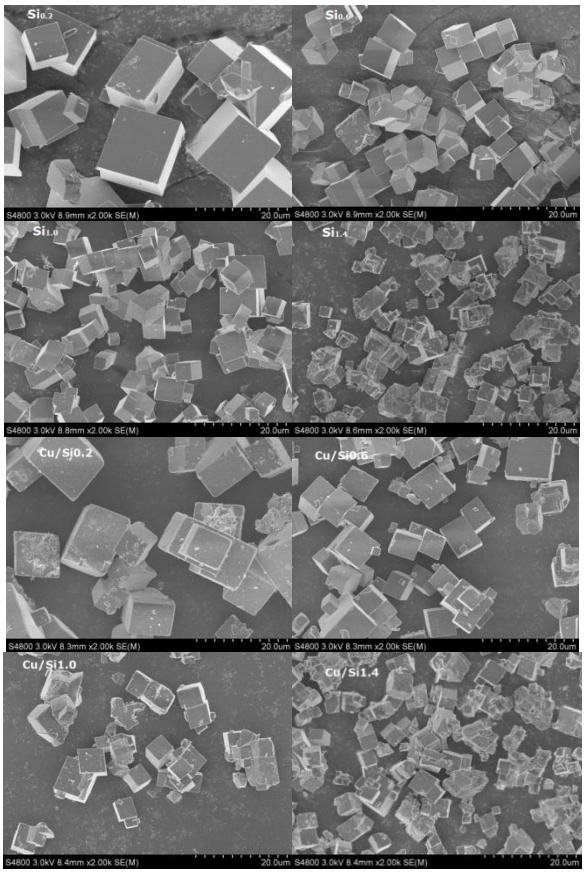

Fig. 2 the SEM images of SAPO-34 supports and Cu/SAPO-34 catalysts

3.2 The NH_3-TPD results

NH_3-TPD is used to research the acidities of zeolites and Fig. 3(a) shows that all the SAPO-34 supports contain three NH_3 desorption peaks, named as A, B and C. Our previous works have reported that the peak (A) arises at the lower temperature related to the weak Brønsted acid sites at surface hydroxyls. The two

View Article Online
DOI: 10.1039/C3CY00453H

peaks (B and C) at the higher temperature are possibly assigned to the structural Brønsted acid sites referred to moderate and strong acidity. In addition, compared to the support the difference of acidic ascription over Cu/SAPO-34 samples is the peak A and C. The peak A of Cu/SAPO-34 samples represents the adsorbed NH_3 molecules at weak Brønsted acid sites and weak Lewis acid sites related to Cu species and the peak C stands for the adsorbed NH_3 molecules both at strong Brønsted acid sites as SAPO-34 supports and new Lewis acid sites created by the Cu species.[10,18,19]. Moreover, the desorbed NH_3 contents in Table 3 illustrate that the increment of Si contents in SAPO-34 can improve their acid contents. The acidity of HSAPO-34 originates from the proton for compensating the unbalanced electronic charges due to Si incorporation into the neutral framework of AlPOs molecular sieves[12,17]. Nevertheless, the acid contents do not scale linearly with the Si amounts, which also illustrate the existence of Si islands. It is known that the Si islands increase with the increment of Si amounts in the four samples.. Furthermore, the structure in Si islands (-Si-O-Si-) could not generate acid sites and the acidity of various Si structures presents the following sequence: Si (1OAl) >Si (2OAl) >Si (3OAl) > Si (4OAl) >Si (0OAl). Consequently, the desorption temperature of peak C moves to higher temperature with the increment of Si amount, which is due to the Si (nOAl, n=0-3) shows the stronger acidity than Si (4OAl) in Si0.2[17].

Table 3 the adsorbed NH_3 contents over SAPO-34 and Cu/SAPO-34 samples

Support	The adsorbed NH_3 contents(mmol/g)	Sample	The adsorbed NH_3 contents(mmol/g)
Si0.2	0.197	Cu/Si0.2	0.075
Si0.6	0.270	Cu/Si0.6	0.195
Si1.0	0.298	Cu/Si1.0	0.202
Si1.4	0.335	Cu/Si1.4	0.243

Fig. 3(b) depicts that the Cu/SAPO-34 also contains three kinds of acid sites. In addition, the sums of adsorbed NH_3 over Cu/SAPO-34 catalysts in Table 3 are less than that of corresponding supports, which is mainly due to the replacement of acid sites (Si-OH-Al) by Cu species[10].

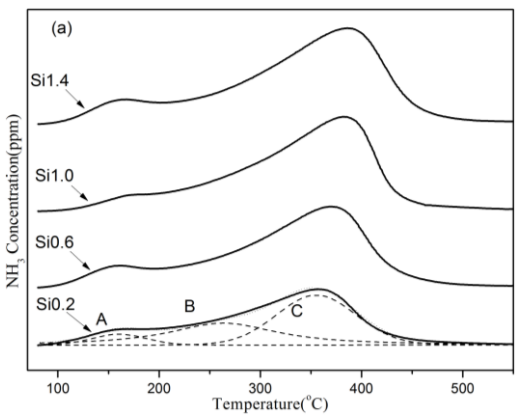

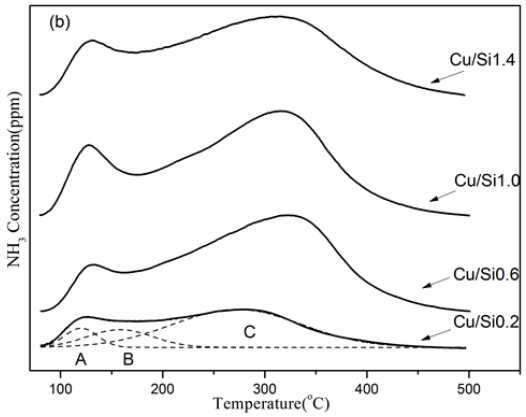

Fig. 3 the NH_3-TPD profiles over (a) SAPO-34 molecular sieves and (b) Cu/SAPO-34 at 80 °C. The conditions were: 500 ppm NH_3 was adsorbed until the outlet NH_3 concentration was stable. The NH_3-TPD experiment was ramped from 80 °C to 550 °C at a rate of 10 °C /min.

3.3 The SCR activities test

The acidity and the loaded Cu species are the main reasons which give Cu/SAPO-34 the excellent SCR performance. Considering the objective of this research, the four Cu/SAPO-34 catalysts comprise the same low Cu loading to emphasize the role of acid contents in NH_3-SCR activities. Fig.4a reveals that the acid contents obviously affect the SCR activities of Cu/SAPO-34 with different Si amounts. Cu/Si1.4 sample performs the best NO conversion, while the Cu/Si0.2 shows the inferior NO conversion. In addition, the Cu/Si0.6 and Cu/Si1.0 have switched SCR activities during middle temperature and high temperature range. The detailed reasons are related to the acid contents discussed later.

The acid contents also influence the side-products of SCR reaction in Fig. 4b. Especially, the Cu/Si0.2 produces 33 ppm N_2O at 295 °C. It is reported that the N_2O formation was due to the decomposition of NH_4NO_3, and the adsorbed NH_3 species could interact with the formed nitrates strongly and this ammonia-nitrates species inhibit the decomposition of formed nitrates for its low acid content[20]. So the highest N_2O production for Cu/Si0.2 sample is due to its lowest adsorbed NH_3 contents for its least acid sites. Other catalysts show excellent N_2 selectivities and the concentrations of NO_2 and N_2O are less than 10 ppm. The NH_3 conversion in Fig. 4c presents the similar sequence with the NO conversion in Fig. 4a, and the NH_3 conversion increases to 100% with the increment of temperature.

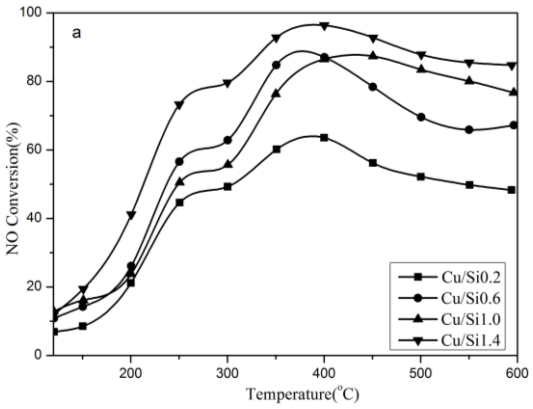

View Article Online
DOI: 10.1039/C3CY00453H

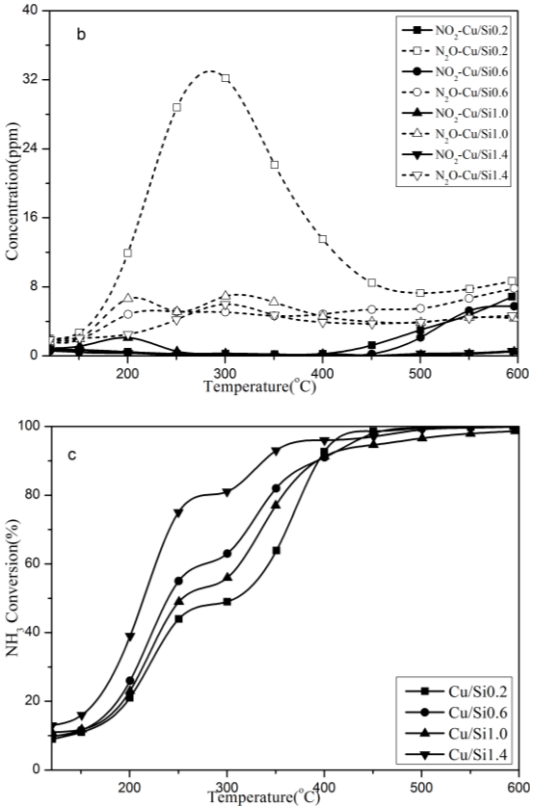

Fig. 4 the results of SCR activities over various Cu/SAPO-34 catalysts. (a) the NO conversion; (b) the concentrations of NO_2、N_2O; (c) the NH_3 conversion. The feed contains 500 ppm NH_3, 500 ppm NO, 5% O_2, N_2 is the balance. The flow rate and the volume hourly space velocity in all experiment were controlled at 500 ml/min and 300,000 h^{-1}

3.4 The SCR activities differences during low temperature range

The NH_3-SCR kinetic tests at low temperature

The SCR results in Fig. 4 reveal completely different NO conversions and Table 1 shows that the main difference among the four Cu/SAPO-34 catalysts with the equivalent Cu loading is the various acid contents. In order to explore the roles of acid contents, the NH_3-SCR kinetic experiments are performed and the results are shown in Fig. 5. Firstly, the NO rates of four catalysts show the same order as the SCR activities in Fig. 4, which explains the differences of NO conversions over various catalysts. Furthermore, the four parallel lines in Fig. 5 reveal that the catalysts have the same apparent activation energy (Ea), which proves that the acid contents do not influence the NH_3-SCR mechanism over Cu/SAPO-34 catalysts.

In addition, the EPR are used to identify the properties of Cu species and the four catalysts contain the same Cu^{2+} species due to the same hyperfine structure in Fig. S3[11]. The results in Fig. S4 (the supplementary information) expose that the Cu^{2+} species are the active sites for NH_3-SCR reaction.

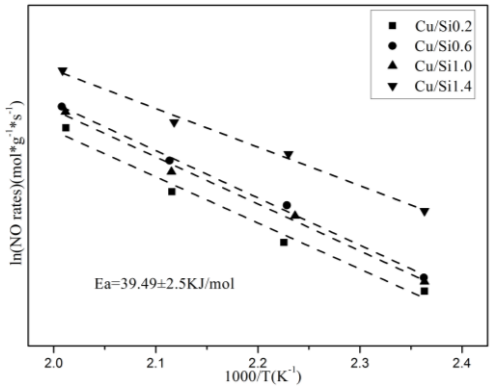

Fig. 5 the kinetic results of NH_3-SCR over Cu/SAPO-34 catalysts at low temperature. The conditions were: the inlets consisted of 500 ppm NO, 500 ppm NH_3, 5% O_2 with N_2 as the balance. The kinetic steady-state measurements were obtained from 150 °C to 225 °C.

The relationship between the acid densities and the activities

To further investigate the influence of the acid contents to the SCR activities, the following experiments about the relation between NH_3 adsorption sum and NO conversion rates at 250 °C were studied and the results are summarized in Fig. 6. Prior to the tests, the catalysts are pretreated in 5% O_2/N_2 and then the ($NO+O_2$) are cut in. When the reaction of ($NO+O_2$) reaches equilibrium, the NH_3 is cut in till stable. Consequently, the stored NH_3 contents can be calculated by subtracting NH_3 contents of outlets from that of inlets. The results in Fig. 6a present the rates of NO conversions increase with the increment of stored NH_3 contents gradually. There are clearly two different steps during the process. It is considered that the NO should be oxidized to nitrate/nitrite to participate in the SCR reaction over Cu/zeolites[2,21,22]. Firstly, when the ($NO+O_2$) attains equilibrium, some nitrate/nitrite species have formed over Cu species. The NH_3 just cut in can react with the formed nitrate/nitrite instantly due to the enough Cu sites for the SCR reaction. When the nitrate/nitrite species are decreasing and the adsorbed NH_3 sum is increasing, the rates of NO conversions slow down till steady state for the coverage of most Cu species by adsorbed NH_3 species. In addition, the Fig. 6a presents that the four catalysts perform the different rates of NO conversions, which reflects that the adsorbed NH_3 sum may be related to their various activities.

After the SCR reaction reaches equilibrium, the adsorbed NH_3 contents are calculated and the results are shown in Fig. 6b. Since the Si contents affect both the SSAs and the acid contents of SAPO-34, the acid densities are used to express the various NH_3 contents over Cu/SAPO-34 catalysts. It is seen that the rates of NO conversions at low temperature are proportion to the acid density of catalysts. Moreover, it is worth to note that the result in Fig. 6 is conducted under the same conditions of SCR performance, which stresses the role of NH_3 adsorption over Cu/SAPO-34. So the NH_3-SCR activity of Cu/SAPO-34 at low temperature is close related with its acid density.

View Article Online
DOI: 10.1039/C3CY00453H

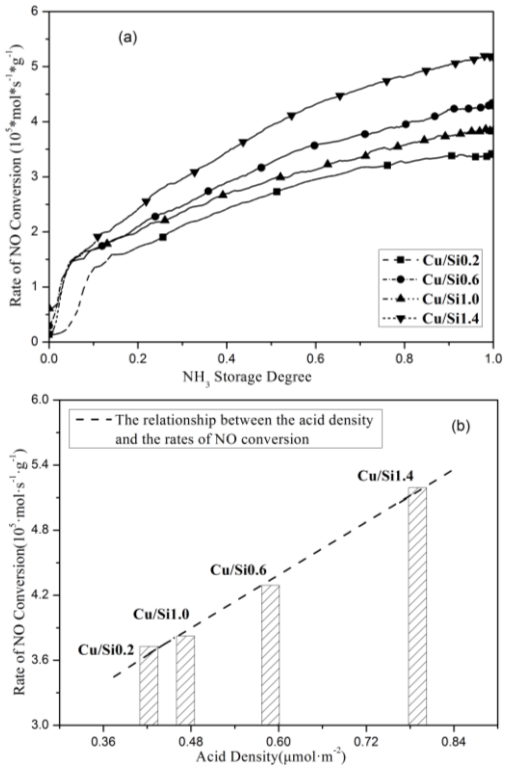

Fig. 6 (a) the relationship between the NH_3 storage and the rate of NO conversion on Cu/SAPO-34 samples at 250 °C. Firstly, the inlets of NO 500 ppm, O_2 5% (vol) attained equilibrium, then the NH_3 500 ppm were cut-in and reach steady. The flow rate is 500 ml/min and the temperature kept at 250 °C. (b) The relationship between the acid density and the rate of NO conversion at 250 °C. The experiments conditions: After the SCR equilibrium was attained on samples at 250 °C, all of the inlets were cutoff except N_2. Then the NH_3-TPD was performed to estimate the adsorbed NH_3 sum. The flow rate is 500 ml/min and the tests were performed at 250 °C. The acid density is the adsorbed NH_3 sum to the SSA ratios for each sample.

3.5 The SCR activities differences during high temperature

The NH_3-SCR kinetic tests at high temperature

The Cu/SAPO-34 catalysts perform the apparently different NO conversions at high temperature in Fig. 4a. In order to identify the possible reasons, the kinetic tests were performed firstly. The kinetic results in Fig. 7 present four parallel lines of NO rates as a function of 1000/T, which illustrates that the same SCR mechanism exists over various catalysts. Furthermore, the results explain the higher NO rates are responsible for the higher NO conversions in Fig. 4a. Furthermore, the different Cu species in the samples are also studied and assigned by H_2-TPR in Fig. S8, and the results in Fig. S9 reveal that the Cu species are not the main reason causing the difference of SCR activity in this research.

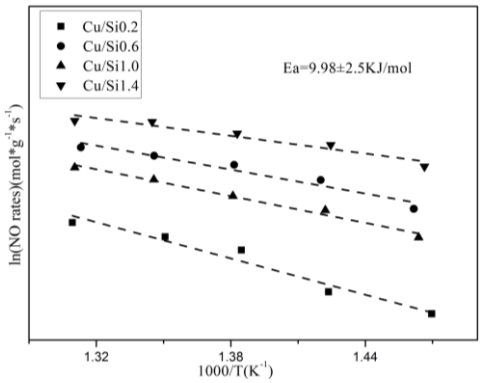

Fig. 7 the NH_3-SCR results under high GHSV (gas hourly space velocity). The conditions were: the inlets consisted of 500 ppm NO, 500 ppm NH_3, 5% O_2 with N_2 as the balance. The kinetic steady-state measurements were obtained from 410 °C to 490 °C.

The NH_3 Oxidation reaction results

It is known that the NH_3 Oxidation and NH_3-SCR are competing relation during SCR process at high temperature[2]. And the NO oxidations over Cu/SAPO-34 present very low NO conversions, which illustrates that the NO oxidation could hardly happen (Fig. 2S in supplementary information). So the NH_3 Oxidation is one of the decisive reasons which cause the decline of the NO conversion at high temperature. The NH_3 oxidation results in Fig. 8a show that the acid contents influence the NH_3 conversions over different catalysts. The Cu/Si0.2 performs the highest NH_3 conversion, while the Cu/Si1.4 shows the lowest NH_3 conversion. It is seen that the increment of acid contents could inhibit the NH_3 oxidation at high temperature. Fig. 8b and 8c expose the side-products of NH_3 oxidation and the concentrations of NO, NO_2 and N_2O. The appearance of NO at high temperature could directly decline the NO conversion for SCR activities. Furthermore, Cu/Si0.6 generates less NO than Cu/Si1.0, which may explain the higher NO rates for the former one than the later in Fig. 7. It is considered that the NH_3 oxidation contained two steps: the NH_3 was oxidized to NO and the formed NO reacted with NH_3 as standard NH_3-SCR reaction[23]. For Cu/Si0.6 and Cu/Si1.0 samples, the former one presents higher NO conversion rate than the later one, so the more NO content is released over Cu/Si1.0 than that over Cu/Si0.6. In addition, the NO_2 and N_2O concentrations in Fig. 8c are much lower than that of NO, but they display the same sequence as byproduct of NO concentrations, which means that the N_2 selectivities and NH_3 conversions in NH_3 oxidation may be affected by the acid contents in catalysts[24].

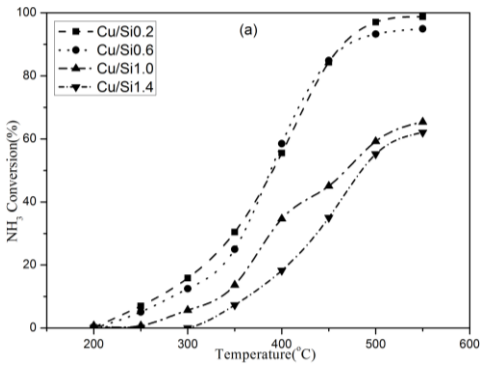

View Article Online
DOI: 10.1039/C3CY00453H

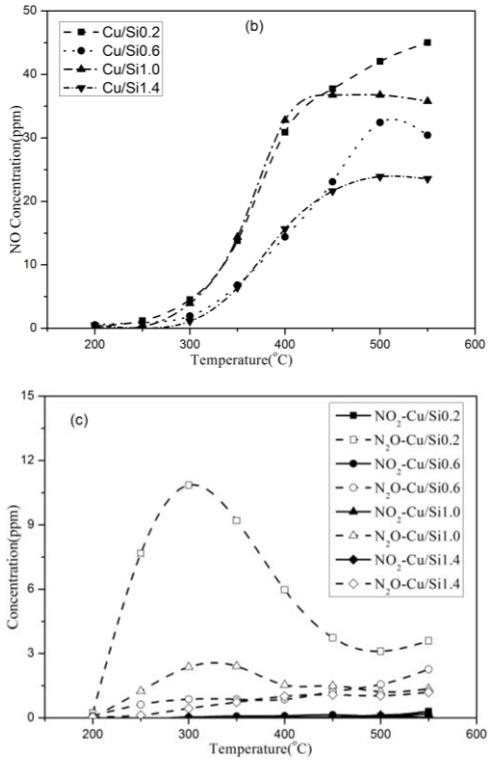

Fig. 8 the NH_3 Oxidation results over Cu/SAPO-34 catalysts. (a) the NH_3 conversion; (b) the NO concentration; (c) the NO_2/N_2O concentration . The conditions were: the inlets consisted of 500 ppm NH_3, 5% O_2 with N_2 as the balance. The flow rate and the volume hourly space velocity in all experiment were controlled at 500 ml/min and 300,000 h^{-1}.

The NH_3 Oxidation kinetic tests

It is seen that the NH_3 Oxidation affect the SCR activities at high temperature. So the kinetic NH_3 Oxidation experiments are conducted to further investigate the influence of acid properties to the SCR activities. Fig. 9 presents the kinetic results of NH_3 oxidations during 410-490 °C, during which the NH_3 conversions are less than 20%. It is seen that the four lines show the similar slopes, which means that the four Cu/SAPO-34 catalysts have the same Ea value for NH_3 oxidation. And the acid contents do not influence the NH_3 oxidation mechanism. Moreover, the NH_3 rates in Fig. 9 present the same sequence of NH_3 conversions in Fig. 8a, which further explain the difference of NH_3 conversions.

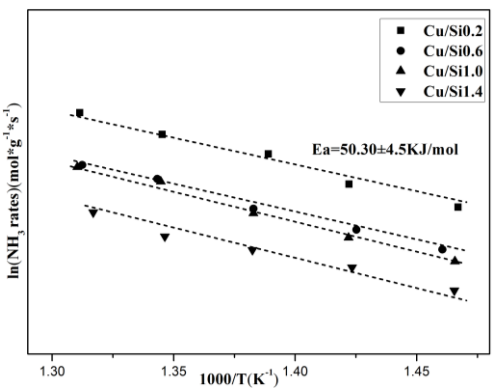

Fig. 9 the NH_3 Oxidation kinetic results over Cu/SAPO-34 catalysts at high temperature. The conditions were: the inlets consisted of 500 ppm NH_3, 5% O_2 with N_2 as the balance. The kinetic steady-state measurements were obtained from 410 °C to 490 °C.

Combining the above data, it is concluded that the SCR activities at high temperature are mainly affected by the competing of NH_3 oxidation for NH_3 consumption. The NH_3-TPD results in Fig. 3 present that only strong acid sites can adsorb NH_3 at high temperature, and the adsorbed NH_3 amounts at different temperature are listed in Table S1 (shown in the supplementary information). It is seen that the adsorbed NH_3 amounts at high temperature increase with the raise of Si contents. Furthermore, the DRIFT results about the different NH_3 behaviour in NH_3-SCR and NH_3 Oxidation at high temperature are conducted in Fig. S5 (supplementary information). The results illustrate that the NH_3 species adsorbed on Cu species (896 cm^{-1}, 840 cm^{-1}) were firstly consumed, while the adsorbed NH_3 species over Bronsted acid sites (3626 cm^{-1}, 3601 cm^{-1}, 3332 cm^{-1}, 3286 cm^{-1}, 1460 cm^{-1}) present different activities in the two reactions. It is concluded that the more strong acid sites is beneficial to NH_3-SCR but not to NH_3 Oxidation on the basis of four catalysts[24,25]. For Cu/Si1.0 sample, though it show lower NO rates for SCR reaction than Cu/Si0.6 in Fig. 7, the later one presents higher NH_3 rates for NH_3 oxidation in Fig. 9. Consequently, the Cu/Si1.0 sample performs better SCR activity than Cu/Si0.6 at high temperature. Moreover, more studies about the effect and the further mechanism researches about the NH_3 oxidation need to been done in future.

4. Conclusions

The four Cu/SAPO-34 catalysts only with various acid contents are used to research the relation between the acid properties and SCR activities. The acid contents of SAPO-34 can be adjusted by the Si amounts and the increment of acid contents improves the NO conversions of Cu/SAPO-34 catalysts.

The acid contents do not affect the apparent activation energy of Cu/SAPO-34 catalysts at low temperature. Meanwhile, the acid density reveals the proportional relation with NO conversion at low temperature.

At high temperature, NH_3-SCR and NH_3 Oxidation are competing relation and the activities of former are mainly influenced by the later one. The acid contents also do not affect the activation energy of NH_3 Oxidation, but the increment of acid content dose not benefit the NH_3 conversion and influences side-products concentrations. The increment of acid contents can inhibit NH_3 oxidation at high temperature.

Acknowledgement

The authors would like to acknowledge GM Global Research & Development (RD-11-368 GB945-NV-HY) for the financial support of this project. This work was also supported by the National High Technology Research and Development Program of China (863 Program, 2011AA03A405).

Notes and references

[a] *Key Laboratory for Green Chemical Technology of State Education Ministry, School of Chemical Engineering & Technology, Tianjin University, Tianjin 300072, China. Tel./ Fax.: +86 22 27892301; E-mail: mqshen@tju.edu.cn*
[b] *State Key Laboratory of Engines, Tianjin University, Tianjin 300072, China*

[c] *General Motors Global Research and Development, Chemical Sciences and Materials Systems Lab, 3500 Mound Road, Warren, MI 48090, USA*

† Electronic Supplementary Information (ESI) available: [Further details are given in Figure S1-S7 and Table S1.]. See DOI: 10.1039/b000000x/

1 J. N. Galloway, F. J. Dentener, D. G. Capone, E. W. Boyer, R. W. Howarth, S. P. Seitzinger, G. P. Asner, C. C. Cleveland, P. A. Green, E. A. Holland, D. M. Karl, A. F. Michaels, J. H. Porter, A. R. Townsend, C. J. Vöosmarty, *Biogeochemistry*, 2004, **70**, 153.

2 G. Busca, L. Lietti, G. Ramis, F. Berti, *Appl. Catal., B*, 1998, **18**, 1.

3 U. Deka, I. Lezcano-Gonzalez, B. M. Weckhuysen, A. M. Beale, *ACS Catal.*, 2013, **3**, 413.

4 D. Wang, L. Zhang, K. Kamasamudram, W. S. Epling, *ACS Catal.*, 2013, **3**, 871.

5 G. Centi, S. Perathoner, *Appl. Catal., A*, 1995, **132**, 179.

6 D.W. Fickel, E. D'Addio, J.A. Lauterbach, R.F. Lobo, *Appl. Catal., B*, 2011, **102**, 441.

7 Y. Jeanvoine, J. G. Ángyán, G. Kresse, J. Hafner, *J. Phys. Chem. B*, 1998, **102**, 5573.

8 J. H. Kwak, R. G. Tonkyn, D. H. Kim, J. Szanyi, C. H. F. Peden, *J. Catal.*, 2010, **275**, 187.

9 J. H. Kwak, D. Tran, S. D. Burton, J. Szanyi, J. H. Lee, C. H. F. Peden, *J. Catal.*, 2012, **287**, 203.

10 J. Wang, T. Yu, X. Wang, G. Qi, J. Xue, M. Shen, W. Li, *Appl. Catal., B*, 2012, **127**, 137.

11 J. Xue, X. Wang, G. Qi, J. Wang, M. Shen, W. Li, *J. Catal.*, 2013, **297**, 56.

12 L. Xu, A. Du, Y. Wei, Y. Wang, Z. Yu, Y. He, X. Zhang, Z. Liu, *Microporous Mesoporous Mater.*, 2008, **115**, 332.

13 L. Marchese, A. Frache, G. Gatti, S. Coluccia, L. Lisi, G. Ruoppolo, G. Russo, H. O. Pastore, *J. Catal.*, 2002, **208**, 479.

14 T. Armaroli, L. J. Simon, M. Digne, T. Montanari, M. Bevilacqua, V. Valtchev, J. Patarin, G. Busca, *Appl. Catal., A*, 2006, **306**, 78.

15 A. L. Villa, C. A. Caro, C. M. d. Correa, *J. Mol. Catal. A: Chem.*, 2005, **228**, 233.

16 A. Izadbakhsh, F. Farhadi, F. Khorasheh, S. Sahebdelfar, M. Asadi, Y. Z. Feng, *Appl. Catal., A*, 2009, **364**, 48.

17 G. Sastre, D. W. Lewis, C. R. A. Catlow, *J. Phys. Chem. B*, 1997, **101**, 5249.

18 S. Ashtekar, S. V. V. Chilukuri, D. K. Chakrabarty, *J. Phys. Chem.*, 1994, **98**, 4878.

19 D. Zhang, Y. Wei, L. Xu, F. Chang, Z. Liu, S. Meng, B.-L. Su, Z. Liu, *Microporous Mesoporous Mater.*, 2008, **116**, 684.

20 A. Grossale, I. Nova, E. Tronconi, *J. Cata.*, 2009, 265, 141.

21 J.-Y. Luo, X. Hou, P. Wijayakoon, S. J. Schmieg, W. Li, W. S. Epling, *Appl. Catal., B*, 2011, **102**, 110.

22 M. Devadas, O. Kröcher, M. Elsener, A. Wokaun, G. Mitrikas, N. Söger, M. Pfeifer, Y. Demel, L. Mussmann, *Catal. Today*, 2007, **119**, 137.

23 G. Qi, J. E. Gatt, R. T. Yang, *J. Cata.*, 2004, 226, 120.

24 H. Zhu, J. H. Kwak, C. H. F. Peden, J. Szanyi, *Catal. Today*, 2013, **205**, 16.

25 R. Q. Long, R. T. Yang, *J. Catal.*, 2001, **201**, 145.

